

Molecular-type $QQss\bar{s}$ pentaquarks predicted by the extended chiral unitary approach

Zhong-Yu Wang^{1,2,*}, Chu-Wen Xiao^{3,4,5,†}, Zhi-Feng Sun^{1,2,6,7,‡} and Xiang Liu^{1,2,6,7,§}

¹*School of Physical Science and Technology, Lanzhou University, Lanzhou 730000, China*

²*Lanzhou Center for Theoretical Physics, Key Laboratory of Theoretical Physics of Gansu Province, and Key Laboratory of Quantum Theory and Applications of the Ministry of Education, Lanzhou University, Lanzhou, 730000, China*

³*Department of Physics, Guangxi Normal University, Guilin 541004, China*

⁴*Guangxi Key Laboratory of Nuclear Physics and Technology, Guangxi Normal University, Guilin 541004, China*

⁵*School of Physics, Central South University, Changsha 410083, China*

⁶*MoE Frontiers Science Center for Rare Isotopes, Lanzhou University, Lanzhou 730000, China*

⁷*Research Center for Hadron and CSR Physics, Lanzhou University and Institute of Modern Physics of CAS, Lanzhou 730000, China*
(Dated: December 27, 2023)

In this work, we investigate the double-heavy molecular pentaquark states with the quark contents $ccss\bar{s}$, $bbss\bar{s}$, and $bcss\bar{s}$ by using the coupled channel approach. The extended local hidden gauge Lagrangians are used to obtain the meson-baryon interactions by exchanging the vector mesons. We predict some candidates for the molecular states with the quantum numbers $I(J^P) = 0(1/2^-, 3/2^-, 5/2^-)$, whose binding energies are of the order of 20–30 MeV and whose widths are all less than 8 MeV. These predicted exotic double-heavy molecular pentaquark states may be accessible in future experiments such as LHCb.

I. INTRODUCTION

How to quantitatively describe the strong interaction at the low energy region is a challenging problem in particle physics. Hadron spectroscopy can provide some insights to deepen our understanding of the non-perturbative behavior of the strong interaction. Usually, there are conventional mesons and baryons, which have the quark components of $q\bar{q}$ and qqq , respectively. These conventional hadrons form the bulk of the reported hadrons, as shown in the Particle Data Group (PDG) [1]. It is the first stage in the construction of the particle zoo.

Since 2003, we have entered a new phase. More and more heavy flavor new hadronic states have been found in experiments, which cannot be explained by the quenched quark model. For example, there were famous low-mass puzzles for these reported $D_{s0}^*(2317)$ [2], $D_{s1}(2460)$ [3], and $X(3872)$ [4]. In 2015, the LHCb Collaboration discovered the pentaquark-like states $P_c(4380)^+$ and $P_c(4450)^+$ in the decay of $\Lambda_b^0 \rightarrow J/\psi K^- p$ [5], which were considered as competing candidates for the hadronic molecular states and attracted intense interest in both theory and experiment. In 2017, the observation of the doubly charmed baryon Ξ_{cc}^{++} in the $\Lambda_c^+ K^- \pi^+ \pi^+$ invariant mass spectrum by the LHCb Collaboration [6] captured the continuing enthusiasm for the heavy states. Furthermore, with the discovery of several narrow states Ω_c [7–10] and Ω_b [11, 12], the LHCb Collaboration tried to search for more doubly heavy baryons, such as Ξ_{bc} , Ω_{cc} , and Ω_{bc} , etc [13]. More results can be found in these recent review articles [14–24]. These new hadronic states not only provide a good opportunity to continue building the particle zoo, but also make it possible to search for exotic states.

In fact, the study of heavy flavor pentaquarks has always

been a focus point in the search for exotic states, as reflected in the recent observations of $P_{cs}(4338)^0$ and $P_{cs}(4459)^0$, which are from the $B^- \rightarrow J/\psi \Lambda \bar{p}$ and $\Xi_b^- \rightarrow J/\psi \Lambda K^-$ processes, respectively [25, 26]. The observation of the characteristic spectrum of $P_c(4312)^+$, $P_c(4440)^+$, and $P_c(4457)^+$ [5, 27] supports the existence of the molecular-type hidden-charm pentaquark [28–33], and other such states were predicted in Refs. [34–37]. The discovered $T_{cc}(3875)$ [38] is a good candidate for a double-charm tetraquark [39–50]. These phenomena mentioned above give us sufficient reason to believe that there should be double-charm molecular pentaquarks [51–56], which is the starting point of the present work.

In this work, we choose a special double-heavy molecular pentaquark system. This system contains most strange quarks. For quantitatively obtaining the information of the mass spectrum of this focused pentaquark system, we adopt an extension of the chiral unitary approach (ChUA) based on the local hidden gauge approach. The ChUA was proposed early on to describe the states $f_0(500)$, $f_0(980)$, $a_0(980)$, and $\Lambda(1405)$ in the molecular configuration [57–63]. Note that the scattering amplitudes of the coupled channels were calculated by solving the Bethe-Salpeter equation using the on-shell approximation in Refs. [58, 59, 63]. This approach has been widely applied in the meson-meson and meson-baryon interactions, with great success, for example in the predictions of the P_c , P_{cs} states [28, 64–66] and the interpretation of the T_{cc} state [67, 68]. Using this approach, Ref. [69] dynamically reproduced three Ω_c states observed in the $\Xi_c^+ K^-$ invariant mass spectrum by the LHCb Collaboration [7]. Moreover, taking the advantage of this method, it has been used to predict the molecular states in the heavy sector, such as the resonances Ω_b [70, 71], Ξ_{cc} [72], Ξ_c and Ξ_b [73], Ξ_{bc} [74], Ξ_{bb} and Ω_{bbb} [75], and so on. Note that the systems with the quark components $ccsq\bar{q}$, $bbssq\bar{q}$, and $bcssq\bar{q}$ were studied in the work of [55], where some states of Ω_{cc} , Ω_{bb} , Ω_{bc} were predicted.

In order to provide more theoretical support to experiment, in the present work we study the double-heavy molecular pentaquark systems with the quark components $ccss\bar{s}$, $bbss\bar{s}$, and $bcss\bar{s}$, which are dynamically generated from the s -wave in-

*Electronic address: zhongyuwang@foxmail.com

†Electronic address: xiaochw@gxnu.edu.cn

‡Electronic address: sunzf@lzu.edu.cn

§Electronic address: xiangliu@lzu.edu.cn

interactions of meson and baryon using an extension of the ChUA based on the local hidden gauge approach. For the meson-baryon interactions, the dominant potentials are obtained by the vector meson exchange mechanism from the extended local hidden gauge Lagrangians as done in Ref. [69]. In fact, the diagonal terms of the matrix for the interaction potentials exchange only the light vector mesons, and thus in the interaction procedures the heavy quarks act as spectators, which automatically respects the heavy quark symmetry. On the other hand, the non-diagonal terms that exchange the heavy vector mesons do not fulfil the heavy quark symmetry, but neither should they since they correspond to subleading terms in the heavy quark counting, see further discussion in Ref. [69].

The rest of the paper is organized as follows. The framework for the potentials of meson-baryon interactions derived from the local hidden gauge Lagrangians is introduced in Sec. II. The numerical results of the scattering amplitudes solved by the coupled channel Bethe-Salpeter equation are presented in Sec. III. Finally, we conclude this work with a summary in Section IV.

II. THE MOLECULAR-TYPE DOUBLE-HEAVY PENTAQUARKS WITH THREE STRANGE QUARKS

In this section, we will briefly introduce the formalism. First, following Ref. [55], we construct the coupled channels of the systems with the quark components $ccss\bar{s}$, $bbss\bar{s}$, and $bcss\bar{s}$.

In the $ccss\bar{s}$ sector, We divide the coupled channels into four blocks, $PB(1/2^+)$, $PB(3/2^+)$, $VB(1/2^+)$, and $VB(3/2^+)$, as shown in Table I, where P stands for the pseudoscalar meson, V for the vector meson, $B(1/2^+)$ for the $J^P = 1/2^+$ ground state baryons, and $B(3/2^+)$ for the $J^P = 3/2^+$ ground state baryons. Note that there is no channel containing the η meson as well as the quark components $ccsq\bar{q}$ ($q = u, d$), as these systems were studied in Ref. [55], and the thresholds are much lower than those of the present work. A similar situation occurs in the $bbss\bar{s}$ and $bcss\bar{s}$ sectors.

The evaluation of the potentials for the meson-baryon interactions is given by the extended local hidden gauge symmetry approach [55]. The interaction mechanism in each block is constructed from the dominant process of the vector meson exchange. The local hidden gauge Lagrangians [76–78] describing the vertices VPP , VVV , and VBB are given by

$$\mathcal{L}_{VPP} = -ig \langle [P, \partial_\mu P] V^\mu \rangle, \quad (1)$$

$$\mathcal{L}_{VVV} = ig \langle (V^\mu \partial_\nu V_\mu - \partial_\nu V^\mu V_\mu) V^\nu \rangle, \quad (2)$$

$$\mathcal{L}_{VBB} = g \langle (\bar{B} \gamma_\mu [V^\mu, B]) + (\bar{B} \gamma_\mu B) \langle V^\mu \rangle \rangle, \quad (3)$$

where g is the coupling constant, which is taken as $M_V/(2f_\pi)$ with M_V the mass of the exchanged light vector meson and $f_\pi = 93$ MeV the pion decay constant. The symbol $\langle \rangle$ denotes the trace of flavor space. Note that Eq. (3) only holds for

TABLE I: Coupled channels in different sectors. The symbol P stands for the pseudoscalar meson, V for the vector meson, $B(1/2^+)$ for the $J^P = 1/2^+$ ground state baryons, and $B(3/2^+)$ for the $J^P = 3/2^+$ ground state baryons.

	$ccss\bar{s}$		$bbss\bar{s}$	
$PB(1/2^+)$	$\eta' \Omega_{cc}$	$D_s \Omega_c$	$\eta' \Omega_{bb}$	$\bar{B}_s \Omega_b$
$PB(3/2^+)$	$\eta' \Omega_{cc}^*$	$D_s \Omega_c^*$	$\eta' \Omega_{bb}^*$	$\bar{B}_s \Omega_b^*$
$VB(1/2^+)$	$\phi \Omega_{cc}$	$D_s^* \Omega_c$	$\phi \Omega_{bb}$	$\bar{B}_s^* \Omega_b$
$VB(3/2^+)$	$\phi \Omega_{cc}^*$	$D_s^* \Omega_c^*$	$\phi \Omega_{bb}^*$	$\bar{B}_s^* \Omega_b^*$
$bcss\bar{s}$				
$PB(1/2^+)$	$\eta' \Omega_{bc}$	$\eta' \Omega'_{bc}$	$D_s \Omega_b$	$\bar{B}_s \Omega_c$
$PB(3/2^+)$	$\eta' \Omega_{bc}^*$	$D_s \Omega_b^*$	$\bar{B}_s \Omega_c^*$	
$VB(1/2^+)$	$\phi \Omega_{bc}$	$\phi \Omega'_{bc}$	$D_s^* \Omega_b$	$\bar{B}_s^* \Omega_c$
$VB(3/2^+)$	$\phi \Omega_{bc}^*$	$D_s^* \Omega_b^*$	$\bar{B}_s^* \Omega_c^*$	

SU(3), light baryons, which is not used in our case, see the discussions later. For the pseudoscalar P and vector V^μ meson fields, they are easily extended from the SU(3) to the SU(5) case following the work of [51, 79],

$$P = \begin{pmatrix} \frac{\eta}{\sqrt{3}} + \frac{\eta'}{\sqrt{6}} + \frac{\pi^0}{\sqrt{2}} & \pi^+ & K^+ & \bar{D}^0 & B^+ \\ \pi^- & \frac{\eta}{\sqrt{3}} + \frac{\eta'}{\sqrt{6}} - \frac{\pi^0}{\sqrt{2}} & K^0 & D^- & B^0 \\ K^- & \bar{K}^0 & -\frac{\eta}{\sqrt{3}} + \sqrt{\frac{2}{3}}\eta' & D_s^- & B_s^0 \\ D^0 & D^+ & D_s^+ & \eta_c & B_c^+ \\ B^- & \bar{B}^0 & \bar{B}_s^0 & \bar{B}_c^- & \eta_b \end{pmatrix}, \quad (4)$$

$$V^\mu = \begin{pmatrix} \frac{\omega + \rho^0}{\sqrt{2}} & \rho^+ & K^{*+} & \bar{D}^{*0} & B^{*+} \\ \rho^- & \frac{\omega - \rho^0}{\sqrt{2}} & K^{*0} & D^{*-} & B^{*0} \\ K^{*-} & \bar{K}^{*0} & \phi & D_s^{*-} & B_s^{*0} \\ D^{*0} & D^{*+} & D_s^{*+} & J/\psi & B_c^{*+} \\ B^{*-} & \bar{B}^{*0} & \bar{B}_s^{*0} & B_c^{*-} & \Upsilon \end{pmatrix}, \quad (5)$$

but one is not making use of SU(5) symmetry, only of the $q\bar{q}$ character of the mesons, as shown in Ref. [80].

We can easily obtain the VPP and VVV vertices in the charm and bottom sectors from Eqs. (1)-(2) and (4)-(5). However, it cannot directly extend the SU(3) VBB vertex to the charm and bottom sectors. According to Ref. [69], the VBB vertex can be constructed through the flavor and spin wave functions of mesons and baryons. In Table II, we list the flavor and spin wave functions of baryons used in this work, following the convention of Ref. [81]. Thus, for the $J^P = 1/2^+$ ground state baryons in the case of $S_z = +1/2$ we have

$$\chi_{MS}(12) = \frac{1}{\sqrt{6}}(\uparrow\downarrow\uparrow + \downarrow\uparrow\uparrow - 2\uparrow\uparrow\downarrow), \quad (6)$$

$$\chi_{MS}(23) = \frac{1}{\sqrt{6}}(\uparrow\downarrow\uparrow + \uparrow\uparrow\downarrow - 2\downarrow\uparrow\uparrow), \quad (7)$$

TABLE II: Wave functions for baryons with $I(J^P) = 0(\frac{1}{2}^+)$ and $0(\frac{3}{2}^+)$, where χ_{MS} stands for mixed symmetric, χ_{MA} stands for mixed anti-symmetric, and χ_S stands for fully symmetric.

States	$I(J^P)$	Flavor	Spin
Ω_{cc}^+	$0(\frac{1}{2}^+)$	ccs	$\chi_{MS}(12)$
Ω_c^0	$0(\frac{1}{2}^+)$	css	$\chi_{MS}(23)$
Ω_{bb}^-	$0(\frac{1}{2}^+)$	bbs	$\chi_{MS}(12)$
Ω_b^-	$0(\frac{1}{2}^+)$	bss	$\chi_{MS}(23)$
Ω_{bc}^0	$0(\frac{1}{2}^+)$	$\frac{1}{\sqrt{2}}b(cs - sc)$	$\chi_{MA}(23)$
$\Omega_{bc}'^0$	$0(\frac{1}{2}^+)$	$\frac{1}{\sqrt{2}}b(cs + sc)$	$\chi_{MS}(23)$
Ω_{cc}^{*+}	$0(\frac{3}{2}^+)$	ccs	χ_S
Ω_c^{*0}	$0(\frac{3}{2}^+)$	css	χ_S
Ω_{bb}^{*-}	$0(\frac{3}{2}^+)$	bbs	χ_S
Ω_b^{*-}	$0(\frac{3}{2}^+)$	bss	χ_S
Ω_{bc}^{*0}	$0(\frac{3}{2}^+)$	$\frac{1}{\sqrt{2}}b(cs + sc)$	χ_S

$$\chi_{MA}(23) = \frac{1}{\sqrt{2}}(\uparrow\uparrow\downarrow - \uparrow\downarrow\uparrow). \quad (8)$$

Note that with our spin independent interaction, for the spin overlap between some baryons, we need the following formulae

$$\langle\chi_{MS}(12)|\chi_{MS}(23)\rangle = -\frac{1}{2}, \quad (9)$$

$$\langle\chi_{MS}(12)|\chi_{MA}(23)\rangle = -\frac{\sqrt{3}}{2}. \quad (10)$$

Furthermore, for the $J^P = 3/2^+$ ground baryon states in the special case $S_z = +3/2$, we obtain

$$\chi_S = \uparrow\uparrow\uparrow. \quad (11)$$

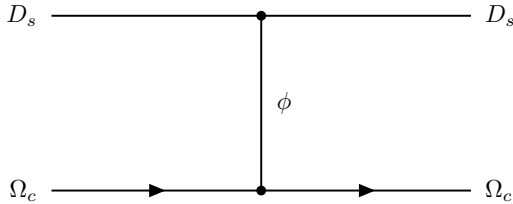


FIG. 1: Diagram of the light vector meson ϕ exchange in the $D_s\Omega_c \rightarrow D_s\Omega_c$ transition.

We can obtain the vertex VBB with the wave functions of the baryons above. Take the $D_s\Omega_c \rightarrow D_s\Omega_c$ process as an example, as shown in Fig. 1, where the interaction of the transition is contributed by the exchange of the light vector meson ϕ in the t -channel. Thus, for the lower vertex we have

$$\langle css\chi_{MS}(23)|gs\bar{s}|css\chi_{MS}(23)\rangle = g. \quad (12)$$

One can see Refs. [72, 80] for more details. More details of the $P_i B_i \rightarrow P_j B_j$ and $V_i B_i \rightarrow V_j B_j$ transitions obtained through two vertices VPP (VVV) and VBB are given in the Appendix of Ref. [69], and we do not repeat them here. Note that we are concerned with the interaction near the threshold, so we have neglected the three-momentum of the external particles in the transitions. Therefore, for the polarizations of the two external vectors, we have $\epsilon_{1\mu}\epsilon_3^{\dagger\mu} = -\vec{\epsilon}_1 \cdot \vec{\epsilon}_3^{\dagger}$ with $\epsilon^0 = 0$.

Finally, the explicit form of the potential from the vector meson exchange mechanism, as shown in Fig. 1, is given by

$$v_{ij} = -C_{ij} \frac{1}{4f_\pi^2} (p_i^0 + p_j^0), \quad (13)$$

where p_i^0 (p_j^0) is the energy of initial (final) meson. The coefficient matrix elements $C_{ij} = C_{ji}$, which are given in Tables III-V. Their relativistically corrected expression in the s -wave is obtained as [82]

$$v_{ij}(\sqrt{s}) = -C_{ij} \frac{2\sqrt{s} - M_i - M_j}{4f_\pi^2} \left(\frac{M_i + E_i}{2M_i} \right)^{1/2} \left(\frac{M_j + E_j}{2M_j} \right)^{1/2}, \quad (14)$$

where M_i (M_j) and E_i (E_j) denote the mass and center-of-mass energy of the initial (final) baryon, respectively.

TABLE III: Coefficient matrix elements C_{ij} in the $ccs\bar{s}\bar{s}$ sector.

	$\eta' \Omega_{cc}$	$D_s \Omega_c$	$\eta' \Omega_{cc}^*$	$D_s \Omega_c^*$
$C_{ij}(PB(1/2^+), PB(3/2^+))$	$\eta' \Omega_{cc}$	0	$\eta' \Omega_{cc}^*$	0
	$D_s \Omega_c$	$\frac{\lambda}{\sqrt{6}}$	$D_s \Omega_c^*$	$\frac{-\sqrt{2}\lambda}{\sqrt{3}}$
$C_{ij}(VB(1/2^+), VB(3/2^+))$	$\phi \Omega_{cc}$	$D_s \Omega_c$	$\phi \Omega_{cc}^*$	$D_s \Omega_c^*$
	$\phi \Omega_{cc}$	0	$\phi \Omega_{cc}^*$	0
	$D_s \Omega_c$	$\frac{\lambda}{2}$	$D_s \Omega_c^*$	$-\lambda$

TABLE IV: Coefficient matrix elements C_{ij} in the $bbs\bar{s}\bar{s}$ sector.

	$\eta' \Omega_{bb}$	$\bar{B}_s \Omega_b$	$\eta' \Omega_{bb}^*$	$\bar{B}_s \Omega_b^*$
$C_{ij}(PB(1/2^+), PB(3/2^+))$	$\eta' \Omega_{bb}$	0	$\eta' \Omega_{bb}^*$	0
	$\bar{B}_s \Omega_b$	0	$\bar{B}_s \Omega_b^*$	0
$C_{ij}(VB(1/2^+), VB(3/2^+))$	$\phi \Omega_{bb}$	$\bar{B}_s \Omega_b$	$\phi \Omega_{bb}^*$	$\bar{B}_s \Omega_b^*$
	$\phi \Omega_{bb}$	0	$\phi \Omega_{bb}^*$	0
	$\bar{B}_s \Omega_b$	0	$\bar{B}_s \Omega_b^*$	0

In Tables III-V, we keep the contributions of the light vector meson and D_s^* meson exchange, ignoring the heavier ones J/ψ , B_s^* , etc. Compared to the light vector mesons, the contribution of exchanging D_s^* meson has a suppression factor of the order of $m_V^2/m_{D_s^*}^2$, i.e., λ , which is approximated as 0.25 in the numerical calculations, see more details in Ref. [69].

With the potentials of the s -wave, one can obtain the scattering amplitudes by solving the Bethe-Salpeter equation with

TABLE V: Coefficient matrix elements C_{ij} in the $bc s \bar{s}$ sector.

	$\eta' \Omega_{bc}$	$\eta' \Omega'_{bc}$	$D_s \Omega_b$	$\bar{B}_s \Omega_c$
$C_{ij}(PB(1/2^+))$	$\eta' \Omega_{bc}$	0	0	0
	$\eta' \Omega'_{bc}$	0	0	$-\frac{2\lambda}{\sqrt{3}}$
	$D_s \Omega_b$	0	$-\frac{2\lambda}{\sqrt{3}}$	1
	$\bar{B}_s \Omega_c$	0	0	0
	$\eta' \Omega_{bc}^*$	$D_s \Omega_b^*$	$\bar{B}_s \Omega_c^*$	
$C_{ij}(PB(3/2^+))$	$\eta' \Omega_{bc}^*$	0	$-\frac{2\lambda}{\sqrt{3}}$	0
	$D_s \Omega_b^*$	$-\frac{2\lambda}{\sqrt{3}}$	1	0
	$\bar{B}_s \Omega_c^*$	0	0	1
	$\phi \Omega_{bc}$	$\phi \Omega'_{bc}$	$D_s^* \Omega_b$	$\bar{B}_s^* \Omega_c$
$C_{ij}(VB(1/2^+))$	$\phi \Omega_{bc}$	0	0	0
	$\phi \Omega'_{bc}$	0	0	$-\sqrt{2}\lambda$
	$D_s^* \Omega_b$	0	$-\sqrt{2}\lambda$	1
	$\bar{B}_s^* \Omega_c$	0	0	0
	$\phi \Omega_{bc}^*$	$D_s^* \Omega_b^*$	$\bar{B}_s^* \Omega_c^*$	
$C_{ij}(VB(3/2^+))$	$\phi \Omega_{bc}^*$	0	$-\sqrt{2}\lambda$	0
	$D_s^* \Omega_b^*$	$-\sqrt{2}\lambda$	1	0
	$\bar{B}_s^* \Omega_c^*$	0	0	1

the on-shell approximation [59], given by

$$T = [1 - vG]^{-1}v. \quad (15)$$

The elements of the diagonal matrix G in Eq. (15) are the loop functions of intermediate mesons and baryons, whose the expression is given by

$$G_l = i \int \frac{d^4 q}{(2\pi)^4} \frac{2M_l}{(P - q)^2 - M_l^2 + i\epsilon} \frac{1}{q^2 - m_l^2 + i\epsilon}, \quad (16)$$

where $P = k_1 + p_1$ is the total momentum of the meson and baryon coupled system. The loop function of Eq. (16) is logarithmically divergent, and therefore it should be regularized, *i.e.*, using the regularization of the three-momentum cutoff method [59], one obtains

$$G_l(s) = \int_0^{q_{max}} \frac{q^2 dq}{2\pi^2} \frac{1}{2\omega_l(q)} \frac{M_l}{E_l(q)} \frac{1}{p^0 + k^0 - \omega_l(q) - E_l(q) + i\epsilon}, \quad (17)$$

where we define $p^0 + k^0 = \sqrt{s}$, $\omega_l(q) = \sqrt{q^2 + m_l^2}$, and $E_l(q) = \sqrt{q^2 + M_l^2}$, with m_l and M_l the masses of meson and baryon of the l channel, respectively, and q_{max} the free parameter. Furthermore, the divergence can also be treated with the

dimensional regularization scheme [63, 83], having

$$G_l(s) = \frac{2M_l}{16\pi^2} \left\{ a(\mu) + \ln \frac{M_l^2}{\mu^2} + \frac{m_l^2 - M_l^2 + s}{2s} \ln \frac{m_l^2}{M_l^2} \right. \\ \left. + \frac{q_{cml}(s)}{\sqrt{s}} \left[\ln \left(s - (M_l^2 - m_l^2) + 2q_{cml}(s)\sqrt{s} \right) \right. \right. \\ \left. \left. + \ln \left(s + (M_l^2 - m_l^2) + 2q_{cml}(s)\sqrt{s} \right) \right. \right. \\ \left. \left. - \ln \left(-s - (M_l^2 - m_l^2) + 2q_{cml}(s)\sqrt{s} \right) \right. \right. \\ \left. \left. - \ln \left(-s + (M_l^2 - m_l^2) + 2q_{cml}(s)\sqrt{s} \right) \right] \right\}. \quad (18)$$

Here, μ is the regularization scale, $a(\mu)$ the subtraction constant, and $q_{cml}(s)$ the three momentum of the particle in the center-of-mass frame, given by

$$q_{cml}(s) = \frac{\lambda^{1/2}(s, M_l^2, m_l^2)}{2\sqrt{s}} \quad (19)$$

with the usual Källén triangle function $\lambda(a, b, c) = a^2 + b^2 + c^2 - 2(ab + ac + bc)$. In the present work, we will use the dimensional regularization scheme. The parameter of μ is chosen as $\mu = q_{max} = 650$ MeV, which is given in Ref. [69] by reproducing the three Ω_c states found in Ref. [7]. And $a(\mu)$ is determined by matching the values of $G_l(s)$ function from these two methods at the threshold, as in Ref. [82].

In the ChUA, to search for the pole, one must extrapolate the $G_l(s)$ function into the second Riemann sheet for $\text{Re}(\sqrt{s})$ being greater than the threshold of the l channel (m_{th}), given by

$$G_l^{(II)}(s) = G_l(s) - 2i\text{Im}G_l(s) \\ = G_l(s) + \frac{i}{2\pi} \frac{M_l q_{cml}(s)}{\sqrt{s}}. \quad (20)$$

Thus, $G_l^{(II)}(s)$ is taken when $\text{Re}(\sqrt{s}) \geq m_{th}$, where the corresponding channel is open for the decay channel, see the results later. Note that the poles on the real energy axis and below the threshold on the first Riemann sheet are bound states. In the coupled channels approach, the quasi-bound states appear as poles off the real energy axis on the unphysical Riemann sheet.

In addition, the coupling constants g_i can be calculated from the Laurent expansion of the amplitudes near the pole $\sqrt{s_p}$ for different channels [84], written as

$$T_{ij} = \frac{g_i g_j}{\sqrt{s} - \sqrt{s_p}}. \quad (21)$$

III. NUMERICAL RESULTS

Table VI shows the thresholds of different channels. The meson and baryon masses used in the calculations are taken from Refs. [1, 53, 85]. In Tables VII-IX, we list the pole positions and their coupling constants for each channel. In brackets after the values of the pole position, the + sign indicates that the corresponding channel is closed, and the - sign

indicates that the corresponding channel is open. The largest coupling constant is highlighted in bold. As mentioned in the previous section, we take the free parameter $\mu = 650$ MeV for all systems.

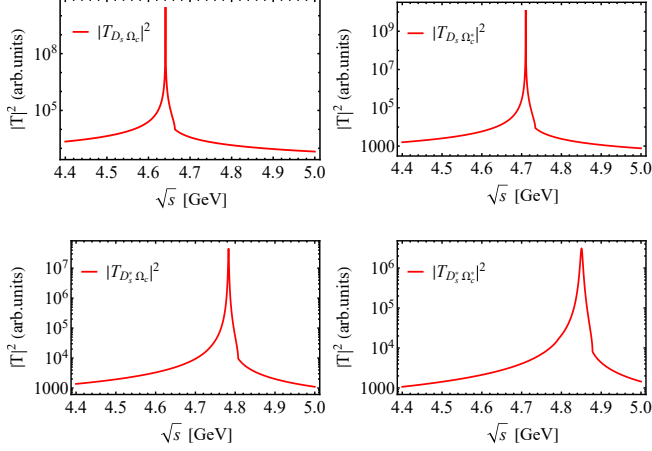


FIG. 2: Modulus square of the amplitudes in the $ccs\bar{s}$ sector, where the ordinate is a logarithmic coordinate system.

First, in Fig. 2, we have plotted the modulus square of the amplitudes $|T|^2$ of the diagonal matrix elements in the $ccs\bar{s}$ system, where four peak structures are clearly visible. Correspondingly, we find four poles on the complex Riemann sheet, which are listed in Table VII. The first two poles 4640.95 MeV and 4710.21 MeV are located on the first Riemann sheet without imaginary parts, indicating that the widths of these two states are zero and that these two states cannot decay into their coupled channel. They are mainly coupled to the $D_s\Omega_c$ channel with quantum number $I(J^P) = 0(1/2^-)$ and the $D_s^*\Omega_c^*$ channel with $I(J^P) = 0(3/2^-)$, respectively, where the first state could mostly qualify as a $D_s\Omega_c$ molecule and the second one as a $D_s^*\Omega_c^*$ molecule, and both of them with a binding of about 23 – 24 MeV. The latter two poles are around 24 – 27 MeV below the thresholds of the most relevant channels, which are found on the second Riemann sheet and the bound states of the $D_s^*\Omega_c$ and $D_s^*\Omega_c^*$ channels, respectively, with the widths of twice the imaginary part of the pole. These two resonances can decay separately into the open channels $\phi\Omega_{cc}$ and $\phi\Omega_{cc}^*$.

Note that Ref. [51] found a state located at 4571 MeV with a width of 90 MeV and mainly coupled to the $D_s\Omega_c$ channel based on the interactions from the chiral effective Lagrangians. As commented in Ref. [86], the subtraction scales μ used in Ref. [51] is unreasonably large to ensure that the heavy channel has a negligible effect on the low-energy scattering of the light channel. In Ref. [54] four states with binding energies around 0.1 MeV to 15 MeV were found with single channel interactions based on the interactions from the heavy quark spin symmetry. The binding energies of the bound states obtained by us are slightly higher than theirs. A main reason for this is that we use the regularization scale $\mu = 650$ MeV in the model, which is obtained by fitting the experimental data in Ref. [69]. In addition, the one-boson-exchange model was used to study the mass spectra of the

$D_s^*\Omega_c^{(*)}$ -type molecular states in Ref. [56], where they obtained similar results using a slightly larger cutoff Λ in the calculations.

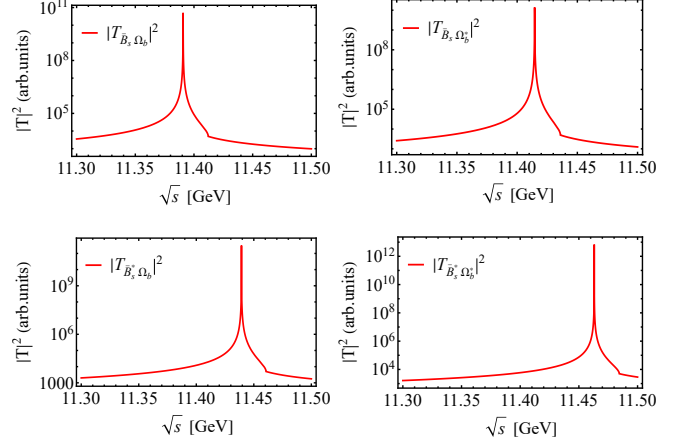


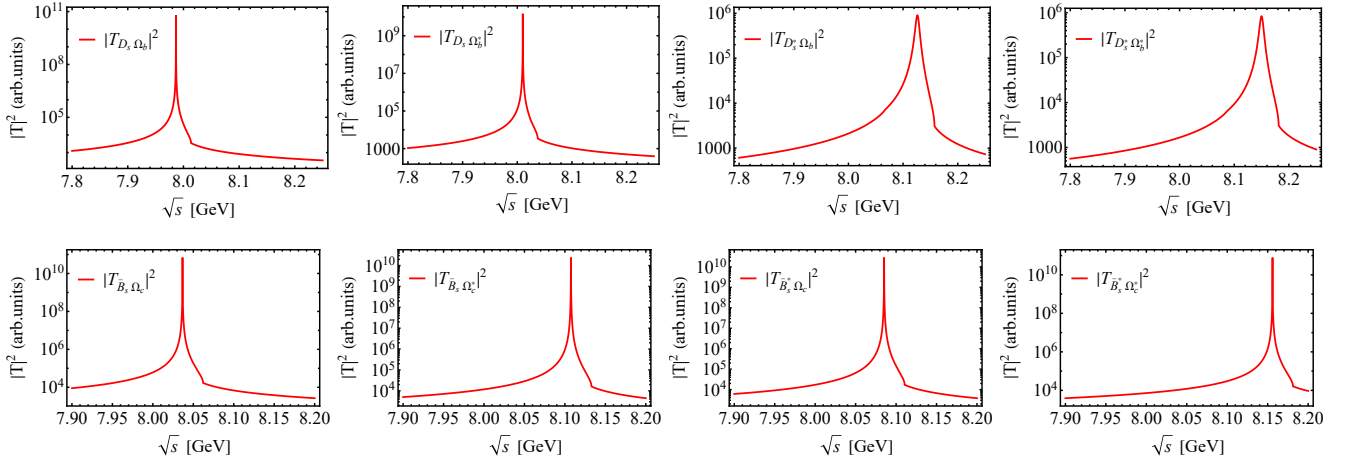
FIG. 3: Modulus square of amplitudes in the $bbss\bar{s}$ sector.

Next, in the $bbss\bar{s}$ sector, we show our results in Fig. 3. From the modulus square of the amplitudes we can see four distinct peaks around the energy range 11380 MeV to 11480 MeV. The poles and their coupling constants for each coupled channel are given in Table VIII. The four states obtained are the $\bar{B}_s\Omega_b$, $\bar{B}_s^*\Omega_b^*$, $\bar{B}_s^*\Omega_b$, and $\bar{B}_s^*\Omega_b^*$ bound states, respectively, which are all found on the first Riemann sheet. Due to the absence of the exchange of light pseudoscalar and B_s^* mesons, which means that there are no coupled channels for each other, see the coefficients in Table IV, the obtained poles are all without imaginary parts. The thresholds of the $\bar{B}_s\Omega_b$, $\bar{B}_s^*\Omega_b^*$, $\bar{B}_s^*\Omega_b$, and $\bar{B}_s^*\Omega_b^*$ channels are 11412.12 MeV, 11435.92 MeV, 11460.60 MeV, and 11484.40 MeV, respectively, see Table VI, and so we have these states all bound at about 21 MeV.

Finally, there are eight bound states in the $bcss\bar{s}$ sector, as shown in Fig. 4 and Table IX. In the case of $PB(1/2^+)$, two poles couple most strongly to the channels $D_s\Omega_b$ and $\bar{B}_s\Omega_c$, with the binding energies 27 MeV and 25 MeV, respectively. In the case of $PB(3/2^+)$, the pole at 8010.12 MeV would be mostly a $D_s\Omega_b^*$ bound state with a binding energy of 27 MeV, and the pole at 8107.45 MeV would be mostly a $\bar{B}_s^*\Omega_c^*$ state bound at 25 MeV. Note that these states have no width, although for the last one, 8107.45 MeV, there may be two lower channels open that are not coupled to the $\bar{B}_s\Omega_c^*$ channel. The two states obtained in the case of $VB(1/2^+)$ sector degenerate in $J^P = 1/2^-$ and $J^P = 3/2^-$. The one of 8126.30 – 3.82i MeV is a molecule of $D_s^*\Omega_b$ and can decay into the open channel $\phi\Omega_{bc}^*$. The other one of 8085.20 MeV is a molecule of $\bar{B}_s^*\Omega_c$ with zero width, which is not coupled to the other channels in this sector. Furthermore, the two states obtained in the case of the $VB(3/2^+)$ sector degenerate in $J^P = 1/2^-, 3/2^-,$ and $5/2^-$. The state 8150.07 – 3.97i MeV is located below the threshold of the most relevant channel $D_s^*\Omega_b^*$ with the largest coupling constant $|g_{D_s^*\Omega_b^*}| = 1.91$, where its binding energy is 31 MeV, and the decay channel is $\phi\Omega_{bc}^*$. The last state in Table IX can be considered as a $\bar{B}_s^*\Omega_c^*$ bound state with a binding energy of

TABLE VI: Thresholds (in MeV) of the relevant channels.

<i>ccss</i> \bar{s}								
Channels	$\eta' \Omega_{cc}$	$D_s \Omega_c$	$\eta' \Omega_{cc}^*$	$D_s \Omega_c^*$	$\phi \Omega_{cc}$	$D_s^* \Omega_c$	$\phi \Omega_{cc}^*$	$D_s^* \Omega_c^*$
Thresholds	4672.78	4663.55	4729.78	4734.25	4734.46	4807.40	4791.46	4878.10
<i>bbss</i> \bar{s}								
Channels	$\eta' \Omega_{bb}$	$\bar{B}_s \Omega_b$	$\eta' \Omega_{bb}^*$	$\bar{B}_s \Omega_b^*$	$\phi \Omega_{bb}$	$\bar{B}_s^* \Omega_b$	$\phi \Omega_{bb}^*$	$\bar{B}_s^* \Omega_b^*$
Thresholds	11187.78	11412.12	11215.78	11435.92	11249.46	11460.60	11277.46	11484.40
<i>bcss</i> \bar{s}								
Channels	$\eta' \Omega_{bc}$	$\eta' \Omega_{bc}'$	$D_s \Omega_b$	$\bar{B}_s \Omega_c$	$\eta' \Omega_{bc}^*$	$D_s \Omega_b^*$	$\bar{B}_s \Omega_c^*$	
Thresholds	7968.78	8004.78	8013.55	8062.12	8023.78	8037.35	8132.82	
Channels	$\phi \Omega_{bc}$	$\phi \Omega_{bc}'$	$D_s^* \Omega_b$	$\bar{B}_s^* \Omega_c$	$\phi \Omega_{bc}^*$	$D_s^* \Omega_b^*$	$\bar{B}_s^* \Omega_c^*$	
Thresholds	8030.46	8066.46	8157.40	8110.60	8085.46	8181.20	8181.30	

FIG. 4: Modulus square of amplitudes in the *bcss* \bar{s} sector.TABLE VII: Poles (in MeV) and their couplings for each channel in the *ccss* \bar{s} sector. The sign + indicates the corresponding channel is closed, and the sign – indicates that the corresponding channel is open, in the same order as the channels in Table I. The largest coupling constant is highlighted in bold.

$I(J^P)$	Poles position	Couplings
$0(\frac{1}{2}^-)$	4640.95 (++)	$ g_{\eta' \Omega_{cc}} = 0.16$ $ g_{D_s \Omega_c} = \mathbf{2.18}$
$0(\frac{3}{2}^-)$	4710.21 (++)	$ g_{\eta' \Omega_{cc}^*} = 0.32$ $ g_{D_s \Omega_c^*} = \mathbf{2.17}$
$0(\frac{1}{2}^-, \frac{3}{2}^-)$	4783.23 – 0.74i (–+)	$ g_{\phi \Omega_{cc}} = 0.21$ $ g_{D_s^* \Omega_c} = \mathbf{2.24}$
$0(\frac{1}{2}^-, \frac{3}{2}^-, \frac{5}{2}^-)$	4850.69 – 3.01i (–+)	$ g_{\phi \Omega_{cc}^*} = 0.39$ $ g_{D_s^* \Omega_c^*} = \mathbf{2.30}$

25 MeV and the coupling $|g_{\bar{B}_s^* \Omega_c^*}| = 2.60$, which has also no width since there are no coupled channels to decay to.

Note that for the molecular states obtained above, the attractions of their most relevant channels are provided by the exchange of the vector meson ϕ , while the interactions in non-

TABLE VIII: Poles (in MeV) and their couplings for every channel in the *bbss* \bar{s} sector.

$I(J^P)$	Poles position	Couplings	
$0(\frac{1}{2}^-)$	11390.73 (++)	$ g_{\eta' \Omega_{bb}} = 0.00$	$ g_{\bar{B}_s \Omega_b} = \mathbf{1.77}$
$0(\frac{3}{2}^-)$	11414.56 (++)	$ g_{\eta' \Omega_{bb}^*} = 0.00$	$ g_{\bar{B}_s \Omega_b^*} = \mathbf{1.77}$
$0(\frac{1}{2}^-, \frac{3}{2}^-)$	11439.27 (++)	$ g_{\phi \Omega_{bb}} = 0.00$	$ g_{\bar{B}_s^* \Omega_b} = \mathbf{1.77}$
$0(\frac{1}{2}^-, \frac{3}{2}^-, \frac{5}{2}^-)$	11463.09 (++)	$ g_{\phi \Omega_{bb}^*} = 0.00$	$ g_{\bar{B}_s^* \Omega_b^*} = \mathbf{1.77}$

diagonal terms are weaker due to the exchange of the heavy vector meson D_s^* . It is very interesting that in the absence of long-range interactions mediated by the exchange of π meson, the bound states can only be formed by the exchange of the heavier meson ϕ . These types of doubly heavy pentaquarks with the most strange quark contents *ccss* \bar{s} , *bbss* \bar{s} , and *bcss* \bar{s} are excellent systems to validate this mechanism. We look forward to the experimental search for these states to

TABLE IX: Poles (in MeV) and their couplings for every channel in the $bc\bar{s}s\bar{s}$ sector.

$I(J^P)$	Poles position	Couplings			
$0(\frac{1}{2}^-)$	7986.54 (+ + + +)	$ g_{\eta'\Omega_{bc}} = 0.00$	$ g_{\eta'\Omega_{bc}'} = 0.36$	$ g_{D_s\Omega_b} = \mathbf{1.81}$	$ g_{\bar{B}_s\Omega_c} = 0.00$
	8036.70 (+ + + +)	$ g_{\eta'\Omega_{bc}} = 0.00$	$ g_{\eta'\Omega_{bc}'} = 0.00$	$ g_{D_s\Omega_b} = 0.00$	$ g_{\bar{B}_s\Omega_c} = \mathbf{2.63}$
$0(\frac{3}{2}^-)$	8010.12 (+ + +)	$ g_{\eta'\Omega_{bc}^*} = 0.36$	$ g_{D_s\Omega_b^*} = \mathbf{1.80}$	$ g_{\bar{B}_s\Omega_c^*} = 0.00$	
	8107.45 (+ + +)	$ g_{\eta'\Omega_{bc}^*} = 0.00$	$ g_{D_s\Omega_b^*} = 0.00$	$ g_{\bar{B}_s\Omega_c^*} = \mathbf{2.59}$	
$0(\frac{1}{2}^-, \frac{3}{2}^-)$	8126.30 - 3.82i (- - + +)	$ g_{\phi\Omega_{bc}} = 0.00$	$ g_{\phi\Omega_{bc}'} = 0.41$	$ g_{D_s^*\Omega_b} = \mathbf{1.91}$	$ g_{\bar{B}_s^*\Omega_c} = 0.00$
	8085.20 (+ + + +)	$ g_{\phi\Omega_{bc}} = 0.00$	$ g_{\phi\Omega_{bc}'} = 0.00$	$ g_{D_s^*\Omega_b} = 0.00$	$ g_{\bar{B}_s^*\Omega_c} = \mathbf{2.63}$
$0(\frac{1}{2}^-, \frac{3}{2}^-, \frac{5}{2}^-)$	8150.07 - 3.97i (- + +)	$ g_{\phi\Omega_{bc}^*} = 0.41$	$ g_{D_s^*\Omega_b^*} = \mathbf{1.91}$	$ g_{\bar{B}_s^*\Omega_c^*} = 0.00$	
	8155.95 (+ + +)	$ g_{\phi\Omega_{bc}^*} = 0.00$	$ g_{D_s^*\Omega_b^*} = 0.00$	$ g_{\bar{B}_s^*\Omega_c^*} = \mathbf{2.60}$	

confirm the model used in this paper. If these states exist, it will deepen our understanding of the nonperturbative behavior of the strong interaction.

IV. SUMMARY

In the present work, we make a study of Ω_{cc} , Ω_{bb} , and Ω_{bc} molecular states dynamically generated from the meson-baryon interaction in the charm and bottom sectors. With the extended local hidden gauge approach, we obtain the dominant interactions through the vector meson exchange mechanism, and then calculate the scattering amplitudes by solving the Bethe-Salpeter equation in the on-shell approximation. By searching for poles in the complex energy plane, the masses and widths of the molecular states are determined. We find several candidates for hadronic molecular states with the quark components $cc\bar{s}s\bar{s}$, $bb\bar{s}s\bar{s}$, and $bc\bar{s}s\bar{s}$.

In the $cc\bar{s}s\bar{s}$ sector, we obtain four bound states mainly coupled to the $D_s\Omega_c$, $D_s\Omega_c^*$, $D_s^*\Omega_c$, and $D_s^*\Omega_c^*$ channels, respectively. In the $bb\bar{s}s\bar{s}$ sector, we obtain four bound states mainly coupled to the $\bar{B}_s\Omega_b$, $\bar{B}_s\Omega_b^*$, $\bar{B}_s^*\Omega_b$, and $\bar{B}_s^*\Omega_b^*$ channels, respectively. In the $bc\bar{s}s\bar{s}$ sector, we obtain eight bound states mainly coupled to $D_s\Omega_b$, $\bar{B}_s\Omega_c$, $D_s\Omega_b^*$, $\bar{B}_s\Omega_c^*$, $D_s^*\Omega_b$, $\bar{B}_s^*\Omega_c$, $D_s^*\Omega_b^*$, and $\bar{B}_s^*\Omega_c^*$ channels, respectively. In the cases of the $PB(1/2^+)$, $PB(3/2^+)$, $VB(1/2^+)$, and $VB(3/2^+)$ sectors, which carry the quantum numbers $I(J^P) = 0(1/2^-)$, $0(3/2^-)$, $0(1/2^-, 3/2^-)$, and $0(1/2^-, 3/2^-, 5/2^-)$, respectively. All these states have

very small or zero widths, which are below the threshold of the most dominant channel about 20 – 30 MeV. The LHCb Collaboration is carrying out the relevant measurement and analysis, and these predicted states are likely to be detected in the near future.

Acknowledgements

We would like to thank Fu-Lai Wang and Wen-Fei Wang for valuable discussions, and acknowledge Profs. Eulogio Oset and Kazem Azizi for careful reading the manuscript and useful comments. This work is supported by the China National Funds for Distinguished Young Scientists under Grant No. 11825503, the National Key Research and Development Program of China under Contract No. 2020YFA0406400, the 111 Project under Grant No. B20063, the fundamental Research Funds for the Central Universities under Grant No. lzujbky-2022-sp02, the project for top-notch innovative talents of Gansu province, and the National Natural Science Foundation of China (NSFC) under Grants No. 12247101, 12335001, 11965016, 11705069 and 12047501 (Z.F.S.). This work is also partly supported by the Natural Science Foundation of Changsha under Grants No. kq2208257, the Natural Science Foundation of Hunan province under Grant No. 2023JJ30647, and the NSFC under Grant No. 12365019 (C.W.X.).

- [1] R. L. Workman *et al.* [Particle Data Group], PTEP **2022**, 083C01 (2022)
- [2] B. Aubert *et al.* [BaBar], Phys. Rev. Lett. **90**, 242001 (2003) [arXiv:hep-ex/0304021 [hep-ex]].
- [3] D. Besson *et al.* [CLEO], Phys. Rev. D **68**, 032002 (2003) [erratum: Phys. Rev. D **75**, 119908 (2007)] [arXiv:hep-ex/0305100 [hep-ex]].
- [4] S. K. Choi *et al.* [Belle], Phys. Rev. Lett. **91**, 262001 (2003) [arXiv:hep-ex/0309032 [hep-ex]].
- [5] R. Aaij *et al.* [LHCb], Phys. Rev. Lett. **115**, 072001 (2015)

- [arXiv:1507.03414 [hep-ex]].
- [6] R. Aaij *et al.* [LHCb], Phys. Rev. Lett. **119**, no.11, 112001 (2017) [arXiv:1707.01621 [hep-ex]].
- [7] R. Aaij *et al.* [LHCb], Phys. Rev. Lett. **118**, no.18, 182001 (2017) [arXiv:1703.04639 [hep-ex]].
- [8] J. Yelton *et al.* [Belle], Phys. Rev. D **97**, no.5, 051102 (2018) [arXiv:1711.07927 [hep-ex]].
- [9] R. Aaij *et al.* [LHCb], Phys. Rev. D **104**, no.9, L091102 (2021) [arXiv:2107.03419 [hep-ex]].
- [10] [LHCb], [arXiv:2302.04733 [hep-ex]].

- [11] R. Aaij *et al.* [LHCb], Phys. Rev. Lett. **124**, no.8, 082002 (2020) [arXiv:2001.00851 [hep-ex]].
- [12] V. Matiunin [LHCb], PoS **ICHEP2020**, 485 (2021) [arXiv:2102.03175 [hep-ex]].
- [13] R. Aaij *et al.* [LHCb], Chin. Phys. C **45**, no.9, 093002 (2021) [arXiv:2104.04759 [hep-ex]].
- [14] X. Liu, Chin. Sci. Bull. **59**, 3815-3830 (2014) [arXiv:1312.7408 [hep-ph]].
- [15] A. Hosaka, T. Iijima, K. Miyabayashi, Y. Sakai and S. Yasui, PTEP **2016**, no.6, 062C01 (2016) [arXiv:1603.09229 [hep-ph]].
- [16] H. X. Chen, W. Chen, X. Liu and S. L. Zhu, Phys. Rept. **639**, 1-121 (2016) [arXiv:1601.02092 [hep-ph]].
- [17] J. M. Richard, Few Body Syst. **57**, no.12, 1185-1212 (2016) [arXiv:1606.08593 [hep-ph]].
- [18] R. F. Lebed, R. E. Mitchell and E. S. Swanson, Prog. Part. Nucl. Phys. **93**, 143-194 (2017) [arXiv:1610.04528 [hep-ph]].
- [19] S. L. Olsen, T. Skwarnicki and D. Zieminska, Rev. Mod. Phys. **90**, no.1, 015003 (2018) [arXiv:1708.04012 [hep-ph]].
- [20] F. K. Guo, C. Hanhart, U. G. Meißner, Q. Wang, Q. Zhao and B. S. Zou, Rev. Mod. Phys. **90**, no.1, 015004 (2018) [erratum: Rev. Mod. Phys. **94**, no.2, 029901 (2022)] [arXiv:1705.00141 [hep-ph]].
- [21] Y. R. Liu, H. X. Chen, W. Chen, X. Liu and S. L. Zhu, Prog. Part. Nucl. Phys. **107**, 237-320 (2019) [arXiv:1903.11976 [hep-ph]].
- [22] N. Brambilla, S. Eidelman, C. Hanhart, A. Nefediev, C. P. Shen, C. E. Thomas, A. Vairo and C. Z. Yuan, Phys. Rept. **873**, 1-154 (2020) [arXiv:1907.07583 [hep-ex]].
- [23] L. Meng, B. Wang, G. J. Wang and S. L. Zhu, Phys. Rept. **1019**, 1-149 (2023) [arXiv:2204.08716 [hep-ph]].
- [24] H. X. Chen, W. Chen, X. Liu, Y. R. Liu and S. L. Zhu, Rept. Prog. Phys. **86**, no.2, 026201 (2023) [arXiv:2204.02649 [hep-ph]].
- [25] R. Aaij *et al.* [LHCb], Phys. Rev. Lett. **131**, no.3, 031901 (2023) [arXiv:2210.10346 [hep-ex]].
- [26] R. Aaij *et al.* [LHCb], Sci. Bull. **66**, 1278-1287 (2021) [arXiv:2012.10380 [hep-ex]].
- [27] R. Aaij *et al.* [LHCb], Phys. Rev. Lett. **122**, no.22, 222001 (2019) [arXiv:1904.03947 [hep-ex]].
- [28] J. J. Wu, R. Molina, E. Oset and B. S. Zou, Phys. Rev. Lett. **105**, 232001 (2010) [arXiv:1007.0573 [nucl-th]].
- [29] W. L. Wang, F. Huang, Z. Y. Zhang and B. S. Zou, Phys. Rev. C **84**, 015203 (2011) [arXiv:1101.0453 [nucl-th]].
- [30] Z. C. Yang, Z. F. Sun, J. He, X. Liu and S. L. Zhu, Chin. Phys. C **36**, 6-13 (2012) [arXiv:1105.2901 [hep-ph]].
- [31] X. Q. Li and X. Liu, Eur. Phys. J. C **74**, no.12, 3198 (2014) [arXiv:1409.3332 [hep-ph]].
- [32] R. Chen, X. Liu, X. Q. Li and S. L. Zhu, Phys. Rev. Lett. **115**, no.13, 132002 (2015) [arXiv:1507.03704 [hep-ph]].
- [33] M. Karliner and J. L. Rosner, Phys. Rev. Lett. **115**, no.12, 122001 (2015) [arXiv:1506.06386 [hep-ph]].
- [34] H. X. Chen, W. Chen, X. Liu, T. G. Steele and S. L. Zhu, Phys. Rev. Lett. **115**, no.17, 172001 (2015) [arXiv:1507.03717 [hep-ph]].
- [35] U. Özdem and K. Azizi, Eur. Phys. J. C **78**, no.5, 379 (2018) [arXiv:1803.06831 [hep-ph]].
- [36] M. L. Du, V. Baru, F. K. Guo, C. Hanhart, U.-G. Meißner, J. A. Oller and Q. Wang, Phys. Rev. Lett. **124**, no.7, 072001 (2020) [arXiv:1910.11846 [hep-ph]].
- [37] K. Azizi, Y. Sarac and H. Sundu, Phys. Rev. D **107**, no.1, 014023 (2023) [arXiv:2210.03471 [hep-ph]].
- [38] R. Aaij *et al.* [LHCb], Nature Phys. **18**, no.7, 751-754 (2022) [arXiv:2109.01038 [hep-ex]].
- [39] A. V. Manohar and M. B. Wise, Nucl. Phys. B **399**, 17-33 (1993) [arXiv:hep-ph/9212236 [hep-ph]].
- [40] T. E. O. Ericson and G. Karl, Phys. Lett. B **309**, 426-430 (1993)
- [41] N. A. Tornqvist, Z. Phys. C **61**, 525-537 (1994) [arXiv:hep-ph/9310247 [hep-ph]].
- [42] D. Janc and M. Rosina, Few Body Syst. **35**, 175-196 (2004) [arXiv:hep-ph/0405208 [hep-ph]].
- [43] G. J. Ding, J. F. Liu and M. L. Yan, Phys. Rev. D **79**, 054005 (2009) [arXiv:0901.0426 [hep-ph]].
- [44] R. Molina, T. Branz and E. Oset, Phys. Rev. D **82**, 014010 (2010) [arXiv:1005.0335 [hep-ph]].
- [45] S. Ohkoda, Y. Yamaguchi, S. Yasui, K. Sudoh and A. Hosaka, Phys. Rev. D **86**, 034019 (2012) [arXiv:1202.0760 [hep-ph]].
- [46] N. Li, Z. F. Sun, X. Liu and S. L. Zhu, Phys. Rev. D **88**, no.11, 114008 (2013) [arXiv:1211.5007 [hep-ph]].
- [47] H. Xu, B. Wang, Z. W. Liu and X. Liu, Phys. Rev. D **99**, no.1, 014027 (2019) [erratum: Phys. Rev. D **104**, no.11, 119903 (2021)] [arXiv:1708.06918 [hep-ph]].
- [48] M. Z. Liu, T. W. Wu, M. Pavon Valderrama, J. J. Xie and L. S. Geng, Phys. Rev. D **99**, no.9, 094018 (2019) [arXiv:1902.03044 [hep-ph]].
- [49] L. Tang, B. D. Wan, K. Maltman and C. F. Qiao, Phys. Rev. D **101**, no.9, 094032 (2020) [arXiv:1911.10951 [hep-ph]].
- [50] Z. M. Ding, H. Y. Jiang and J. He, Eur. Phys. J. C **80**, no.12, 1179 (2020) [arXiv:2011.04980 [hep-ph]].
- [51] J. Hofmann and M. F. M. Lutz, Nucl. Phys. A **763**, 90-139 (2005) [arXiv:hep-ph/0507071 [hep-ph]].
- [52] O. Romanets, L. Tolos, C. Garcia-Recio, J. Nieves, L. L. Salcedo and R. G. E. Timmermans, Phys. Rev. D **85**, 114032 (2012) [arXiv:1202.2239 [hep-ph]].
- [53] Q. S. Zhou, K. Chen, X. Liu, Y. R. Liu and S. L. Zhu, Phys. Rev. C **98**, no.4, 045204 (2018) [arXiv:1801.04557 [hep-ph]].
- [54] X. K. Dong, F. K. Guo and B. S. Zou, Commun. Theor. Phys. **73**, no.12, 125201 (2021) [arXiv:2108.02673 [hep-ph]].
- [55] W. F. Wang, A. Feijoo, J. Song and E. Oset, Phys. Rev. D **106**, no.11, 116004 (2022) [arXiv:2208.14858 [hep-ph]].
- [56] F. L. Wang and X. Liu, Phys. Rev. D **108**, no.7, 074022 (2023) [arXiv:2308.15255 [hep-ph]].
- [57] N. Kaiser, P. B. Siegel and W. Weise, Nucl. Phys. A **594**, 325-345 (1995) [arXiv:nucl-th/9505043 [nucl-th]].
- [58] J. A. Oller and E. Oset, Nucl. Phys. A **620**, 438-456 (1997) [erratum: Nucl. Phys. A **652**, 407-409 (1999)] [arXiv:hep-ph/9702314 [hep-ph]].
- [59] E. Oset and A. Ramos, Nucl. Phys. A **635**, 99-120 (1998) [arXiv:nucl-th/9711022 [nucl-th]].
- [60] N. Kaiser, Eur. Phys. J. A **3**, 307-309 (1998).
- [61] J. A. Oller, E. Oset and J. R. Peláez, Phys. Rev. D **59**, 074001 (1999) [erratum: Phys. Rev. D **60**, 099906 (1999); erratum: Phys. Rev. D **75**, 099903 (2007)] [arXiv:hep-ph/9804209 [hep-ph]].
- [62] J. A. Oller, E. Oset and A. Ramos, Prog. Part. Nucl. Phys. **45**, 157-242 (2000) [arXiv:hep-ph/0002193 [hep-ph]].
- [63] J. A. Oller and U.-G. Meißner, Phys. Lett. B **500**, 263-272 (2001) [arXiv:hep-ph/0011146 [hep-ph]].
- [64] J. J. Wu, R. Molina, E. Oset and B. S. Zou, Phys. Rev. C **84**, 015202 (2011) [arXiv:1011.2399 [nucl-th]].
- [65] C. W. Xiao, J. Nieves and E. Oset, Phys. Rev. D **88**, 056012 (2013) [arXiv:1304.5368 [hep-ph]].
- [66] C. W. Xiao, J. Nieves and E. Oset, Phys. Lett. B **799**, 135051 (2019) [arXiv:1906.09010 [hep-ph]].
- [67] A. Feijoo, W. H. Liang and E. Oset, Phys. Rev. D **104**, no.11, 114015 (2021) [arXiv:2108.02730 [hep-ph]].
- [68] L. R. Dai, L. M. Abreu, A. Feijoo and E. Oset, [arXiv:2304.01870 [hep-ph]].
- [69] V. R. Debastiani, J. M. Dias, W. H. Liang and E. Oset, Phys.

- Rev. D **97**, no.9, 094035 (2018) [arXiv:1710.04231 [hep-ph]].
- [70] W. H. Liang, J. M. Dias, V. R. Debastiani and E. Oset, Nucl. Phys. B **930**, 524-532 (2018) [arXiv:1711.10623 [hep-ph]].
 - [71] W. H. Liang and E. Oset, Phys. Rev. D **101**, no.5, 054033 (2020) [arXiv:2001.02929 [hep-ph]].
 - [72] J. M. Dias, V. R. Debastiani, J. J. Xie and E. Oset, Phys. Rev. D **98**, no.9, 094017 (2018) [arXiv:1805.03286 [hep-ph]].
 - [73] Q. X. Yu, R. Pavao, V. R. Debastiani and E. Oset, Eur. Phys. J. C **79**, no.2, 167 (2019) [arXiv:1811.11738 [hep-ph]].
 - [74] Q. X. Yu, J. M. Dias, W. H. Liang and E. Oset, Eur. Phys. J. C **79**, no.12, 1025 (2019) [arXiv:1909.13449 [hep-ph]].
 - [75] J. M. Dias, Q. X. Yu, W. H. Liang, Z. F. Sun, J. J. Xie and E. Oset, Chin. Phys. C **44**, no.6, 064101 (2020) [arXiv:1912.04517 [hep-ph]].
 - [76] M. Bando, T. Kugo, S. Uehara, K. Yamawaki and T. Yanagida, Phys. Rev. Lett. **54**, 1215 (1985).
 - [77] M. Bando, T. Kugo and K. Yamawaki, Phys. Rept. **164**, 217-314 (1988).
 - [78] U.-G. Meißner, Phys. Rept. **161**, 213 (1988).
 - [79] T. Mizutani and A. Ramos, Phys. Rev. C **74**, 065201 (2006) [arXiv:hep-ph/0607257 [hep-ph]].
 - [80] S. Sakai, L. Roca and E. Oset, Phys. Rev. D **96**, no.5, 054023 (2017) [arXiv:1704.02196 [hep-ph]].
 - [81] F. E. Close, "An Introduction to Quarks and Partons", Academic Press, Cambridge, 1979
 - [82] E. Oset, A. Ramos and C. Bennhold, Phys. Lett. B **527**, 99-105 (2002) [erratum: Phys. Lett. B **530**, 260-260 (2002)] [arXiv:nucl-th/0109006 [nucl-th]].
 - [83] D. Jido, J. A. Oller, E. Oset, A. Ramos and U.-G. Meißner, Nucl. Phys. A **725**, 181-200 (2003) [arXiv:nucl-th/0303062 [nucl-th]].
 - [84] J. Yamagata-Sekihara, J. Nieves and E. Oset, Phys. Rev. D **83**, 014003 (2011) [arXiv:1007.3923 [hep-ph]].
 - [85] G. L. Yu, Z. Y. Li, Z. G. Wang, J. Lu and M. Yan, Nucl. Phys. B **990**, 116183 (2023) [arXiv:2206.08128 [hep-ph]].
 - [86] J. A. Marsé-Valera, V. K. Magas and A. Ramos, Phys. Rev. Lett. **130**, no.9, 9 (2023) [arXiv:2210.02792 [hep-ph]].